Nihon Reoroji Gakkaishi Vol.36, No.1, 43~49
(Journal of the Society of Rheology, Japan)

Article

Effects of Interface Velocity on the Stress Tensor in Immiscible Polymer Blends: Retraction of Spheroidal Droplets and Stress Relaxation

Kenzo OKAMOTO*and Masaoki TAKAHASHI**†

*Venture Laboratory, Kyoto Institute of Technology
Matsugasaki, Sakyo-ku, Kyoto 606-8585, Japan
**Department of Macromolecular Science and Engineering, Kyoto Institute of Technology
Matsugasaki, Sakyo-ku, Kyoto 606-8585, Japan
(Received : July 9, 2007)

The total stress tensor for immiscible polymer blends is calculated based on the theoretical expression by Batchelor (1970), and Mellema and Willemse (1983) in the last stage of the stress relaxation under large step shear strains. In this stage, the shape of droplets is spheroid and the retraction of isolated droplets is calculated according to the theory developed by Okamoto et al. (1999). The calculated results are compared with experimental data for a polyisobutylene/ polydimethylsiloxane blend. Contribution of the motion of the interface (the interface velocity term) to the total stress tensor in the theoretical expression for the isolated droplets is 37 % – 50 %, which cannot be neglected compared with the contribution of the pressure difference beyond the interface (the Laplace pressure term). The summation of both terms agrees well with the experimental data at step strain $\gamma = 1$, in which effects inherent in multiple droplet systems are the smallest. The γ dependence of the reduced stress appearing in the experimental data, which cannot be predicted by the theoretical calculation for the isolated droplets, is qualitatively explained by considering droplet size distribution in the theoretical calculation.
Key Words: Stress tensor / Stress relaxation / Polymer blend / Interface velocity / Droplet size distribution

1. INTRODUCTION

There have been many theoretical studies to express the stress tensor due to the interface in mixtures of two fluids under large deformation. The equation proposed by Batchelor[1] and modified by Mellema and Willemse[2] is one of the most general expressions for the stress tensor for mixtures of two Newtonian fluids. They calculated the macroscopic stress tensor from the volume average of the local stress tensor. Their expression includes the contributions from the motion of the interface (the interface velocity term) and the pressure difference beyond the interface (the Laplace pressure term). These terms allow us to evaluate the stress tensor from the velocity and the shape of the interface.

Later, the Laplace pressure term was closely examined. Onuki[3] derived the same expression as the Laplace pressure term for critical binary mixtures. Doi and Ohta[4] used the same expression to calculate the stress tensor for mixtures of Newtonian fluids with equal viscosities and equal volume fractions, and found the scaling relation for the stress tensor. This scaling relation was experimentally examined for mixtures of Newtonian fluids and immiscible polymer blends with various volume fractions, and with equal or different viscosities under shear flow. It was found that the scaling relation works well for the blends with $K \cong 1$[5-7] and $K < 1$[8], where K is the viscosity ratio defined by the ratio of viscosity of droplet phase to that of matrix phase. For the stress relaxation of polymer blends with $K < 1$ under large step shear strains, the Laplace pressure term evaluated from the shape recovery data of isolated droplets agrees fairly well with experimentally obtained stress relaxation data.[9-11]

Recently, the interface velocity term is taken into account in some theories.[12-14] The total stress including the interface velocity and the Laplace pressure terms is compared with literature data of dynamic moduli, steady shear flow and start-up of shear flow for polymer blends.[13] The agreements between the theoretical predictions and the experimental data seem to be well. However, the significance of the interface velocity term compared with the Laplace pressure term is not clear in their studies since the contributions of the two terms are not separately shown.

On the other hand, Yu and Zhou[15] theoretically considered

† To whom correspondence should be addressed.
E-mail: mdt@kit.ac.jp, Tel/Fax: +81-75-724-7835

the effect of the droplet size distribution, and revealed that the droplet size distribution has significant influence on the excess first normal stress difference of polymer blends in start-up of shear flow. Takahashi et al.[10] also reported that the experimental results of the stress relaxation for a hydroxypropylcellulose aqueous solution/polydimethylsiloxane (PDMS) blend agree with the stress calculated by the Laplace pressure term only when the droplet size distribution is considered. In addition, Takahashi and Okamoto[11] speculated that the droplet size distribution affects the strain dependence of the stress relaxation for a polyisobutylene (PIB)/PDMS blend especially for the retraction of spheroidal droplets.

In the present study, we focus on the last stage of the stress relaxation under large step shear strains, in which the shape of the droplets is spheroid. In this stage, the time evolution of the droplet shape is well described by the theory for the retraction of spheroidal droplet.[11,16] Here, we evaluate the interface velocity and the Laplace pressure terms using the time evolution of the droplet shape calculated by this theory. The theoretical predictions are compared with experimental results of the stress relaxation for a PIB/PDMS blend.[9] A merit in treating the last stage is that viscoelasticity of component polymers does not have significant influence on the stress relaxation, and no subtraction procedure for the experimental data is necessary to compare the data with the theoretical predictions since the component polymers relax before this stage. The objective of the present study is to clarify the contribution of the velocity term to the total stress in the last stage. The effect of the droplet size distribution is also considered in the theoretical calculation and is discussed.

2. THEORY

2.1 Contributions of Interface to the Stress Tensor

The stress tensor $\boldsymbol{\sigma}$ for a mixture of two Newtonian fluids at low Reynolds number, where the inertial force is negligible, can be written as follows:[1,2]

$$\boldsymbol{\sigma} = -p\boldsymbol{\delta} + \eta_m\left[\nabla\mathbf{v} + (\nabla\mathbf{v})^T\right] - \frac{(\eta_m - \eta_d)}{V}\int_{S_0} dS(\mathbf{un} + \mathbf{nu}) + \frac{\Gamma}{V}\int_{S_0} dS\left(\frac{1}{3}\boldsymbol{\delta} - \mathbf{nn}\right). \quad (1)$$

Here p is the isotropic part of the stress, $\boldsymbol{\delta}$ the unit tensor, η_m the viscosity of matrix phase, η_d the viscosity of droplet phase, $\nabla\mathbf{v}$ is the velocity gradient tensor, Γ the interfacial tension between two phases, V the total volume of the system, S_0 the total area of the interface, $\mathbf{u}$ the local velocity vector on the interface, and $\mathbf{n}$ the unit outward normal vector on the interface.

The first term in Eq. 1 represents the isotropic pressure. The second term expresses the viscous stress of the matrix fluid without any dispersed phase. The third term (the interface velocity term) is the contribution from the viscous flows of the matrix phase and the dispersed phase due to the local flow caused by the displacement of the interface. The forth term arises from the difference of the normal stress beyond the interface due to the Laplace pressure (the Laplace pressure term), which is given by the following equation:[17,18]

$$\boldsymbol{\sigma}_{m,local}\cdot\mathbf{n} - \boldsymbol{\sigma}_{d,local}\cdot\mathbf{n} = \Gamma(\nabla\cdot\mathbf{n})\,\mathbf{n}, \quad (2)$$

where $\boldsymbol{\sigma}_{m,local}$ and $\boldsymbol{\sigma}_{d,local}$ represent the local stress tensor on the surface at the matrix phase and at the droplet phase, respectively. The forth term in Eq. (1) corresponds to the excess stress due to the interface tensor.[3,4]

For the mixtures of viscoelastic fluids, the other terms, which describe contribution from the viscoelasticity of the fluids, should be added to Eq. (1). In addition, $\mathbf{u}$ may be affected by the viscoelasticity of the fluids.[14] However, we focus only on the last stage of the stress relaxation under large step shear strains in the present study. In this last stage, the matrix and the dispersed phase behave as Newtonian fluids, and only the third and the forth terms in Eq. 1 are significant. Therefore, we simplify Eq. (1) and express the shear stress σ_{xy} during the last stage of the stress relaxation as follows:

$$\sigma_{xy} = \sigma_{v,xy} + \sigma_{L,xy} = -\frac{(\eta_m - \eta_d)}{V}\int_{S_0} dS(u_x n_y + n_x u_y) - \frac{\Gamma}{V}\int_{S_0} dS\, n_x n_y, \quad (3)$$

where $\sigma_{v,xy}$ and $\sigma_{L,xy}$ respectively denote the xy components of the third (the interface velocity) and the fourth (the Laplace pressure) terms in Eq. (1). x and y correspond to the flow direction and the direction of the velocity gradient, respectively (the vorticity direction is denoted by z in the present paper).

In the last stage of the stress relaxation, the shape of droplets is spheroid.[19] Figure 1 shows the droplet shape in the last stage. a, b ($a > b$) and θ respectively denote the length of the semi-major axis, the length of the semi-minor axes and the orientation angle of the droplet. The major stretch ratio λ_a and the minor stretch ratio λ_b of the droplet can be defined by

$$\lambda_a = a/r_0, \quad (4a)$$

$$\lambda_b = b/r_0, \quad (4b)$$

where r_0 represents the radius of the spherical droplet before the deformation. We assume the volume conservation for the droplet, which results in $\lambda_b = \lambda_a^{-1/2}$. In this case, the Laplace pressure term is given by[9,20]

$$\sigma_{L,xy} = \left(\frac{3\Gamma\phi}{8r_0}\right)\sin 2\theta\left[\frac{\lambda_a{}^3+2}{\lambda_a\left(\lambda_a{}^3-1\right)} + \frac{\sqrt{\lambda_a}\left(\lambda_a{}^3-4\right)}{\left(\lambda_a{}^3-1\right)}\times\frac{\arcsin\sqrt{1-\lambda_a{}^{-3}}}{\sqrt{1-\lambda_a{}^{-3}}}\right], \quad (5)$$

where ϕ denotes the volume fraction of the dispersed phase. In the stress relaxation under large step shear strains, θ has been found to be independent of time and equal to the angle given by the affine deformation assumption for mixtures with $0.048 \le K \le 0.54$:[19,21,22]

$$\cot 2\theta = \gamma/2\,. \quad (6)$$

Concerning the interface velocity term, the time evolution of the semi-axes for the ellipsoidal droplet can be written as[12]

$$\frac{D\mathbf{G}}{Dt} + \mathbf{L}^{\mathrm{T}}\cdot\mathbf{G} + \mathbf{G}\cdot\mathbf{L} = 0\,, \quad (7)$$

where **G** describes the shape of the droplet (the shape tensor), **L** the droplet velocity gradient tensor and D/Dt the material derivative. In Cartesian coordinates $\mathbf{X} = (X,Y,Z)$, whose origin and axes respectively coincide with the center and the axes of the ellipsoidal droplet (see Fig. 1), the points on the surface of the droplet satisfy $\mathbf{G}:\mathbf{XX} = 1$,[12] and **G** for the spheroid is given by

$$\mathbf{G} = \begin{pmatrix} a^{-2} & 0 & 0 \\ 0 & b^{-2} & 0 \\ 0 & 0 & b^{-2} \end{pmatrix}. \quad (8)$$

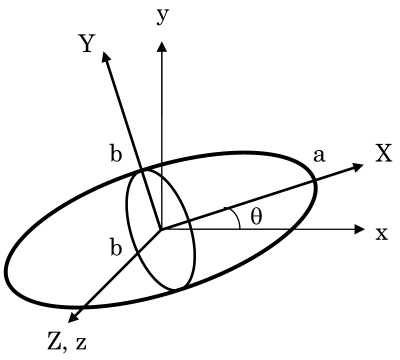

Fig. 1. Cartesian coordinate systems x,y,z and X,Y,Z for a spheroidal droplet with semi axes a,b ($a > b$). The flow direction is x and the direction of velocity gradient is y. θ is the orientation angle.

Since no rotation of the droplet occurs throughout the relaxation process, **L** is considered to be diagonal, and $L_{XX} = d \ln a/dt$ and $L_{YY} = L_{ZZ} = d \ln b/dt$ are obtained from Eqs. (7) and (8).[23] While the velocity field around the droplet is complex, the instantaneous local velocity **u** in the droplet including the interface can be written as

$$\mathbf{u} = \mathbf{R}\cdot\left(\mathbf{L}\cdot\mathbf{X}\right) \quad (9)$$

for ellipsoidal droplets,[12] where **R** represents the tensor of the transformation from the coordinates **X** to $\mathbf{x} = (x,y,z)$.

The unit normal vector **n** can be written as

$$\mathbf{n} = \frac{\mathbf{r}_\Theta \times \mathbf{r}_\Phi}{\left|\mathbf{r}_\Theta \times \mathbf{r}_\Phi\right|}, \quad (10)$$

where $\mathbf{r}_\Theta$ and $\mathbf{r}_\Phi$ are respectively given by $\mathbf{r}_\Theta = \partial\mathbf{r}/\partial\Theta$ and $\mathbf{r}_\Phi = \partial\mathbf{r}/\partial\Phi$ as functions of the parameters Θ and Φ with the position vector $\mathbf{r}(\Theta,\Phi)$ of the points on the spheroid.

From Eqs. (9) and (10), the integration of the interface velocity term in Eq. (3) becomes

$$\sigma_{v,xy} = 3\phi\left(\eta_m - \eta_d\right)\sin 2\theta\; L_{YY}\,, \quad (11)$$

where $V = 4\pi ab^2/(3\phi)$ is used.

2.2 Time Evolution of the Interface Velocity Term $\sigma_{v,xy}$

The viscoelastic relaxation time τ_D of droplets for small deformation is given by[24,25]

$$\tau_D = \frac{r_0\eta_m}{4\Gamma}\frac{\left(19K+16\right)\left(2K+3-2\phi\left(K-1\right)\right)}{10\left(K+1\right)-2\phi\left(5K+2\right)}. \quad (12)$$

For the retraction of isolated droplets, τ_D can be determined by extrapolating $\phi \to 0$.[19] Experimental results show that plots of λ_a versus $(t-t_s)/\tau_D$ make a single curve for the shape retraction of spheroidal droplets independently of r_0 and γ,[11] where t_s is the time at which the shape of the droplets becomes spheroid, and λ_a at $t = t_s$ is experimentally determined as $\lambda_a(t_s) = 1.49$.[19,20] This means that the reduced velocity gradient tensor $\mathbf{\Lambda}$ of isolated droplets, which is independent of r_0 and γ, can be defined as a function of $(t-t_s)/\tau_D$ by

$$\Lambda_{XX} = d\ln\lambda_a/d\left(t/\tau_D\right), \quad (13a)$$

$$\Lambda_{YY} = \Lambda_{ZZ} = d\ln\lambda_b/d\left(t/\tau_D\right). \quad (13b)$$

These definitions lead

$$\mathbf{L} = \mathbf{\Lambda}/\tau_D\,. \quad (14)$$

The time evolution of λ_b can be written as[11,16]

$$\int_{\lambda_b(t_s)}^{\lambda_b(t)} \frac{d\lambda_b}{\lambda_b^{\,3}-\lambda_b^{\,6}} = \frac{t-t_s}{24\chi_0\tau_D}, \quad (15)$$

where χ_0 is the hydrodynamic factor for spheroidal droplets.

The differentiation of both sides of Eq. (15) by t/τ_D leads:

$$\Lambda_{YY} = \frac{\lambda_b^{\,2}-\lambda_b^{\,5}}{24\chi_0} \quad (16)$$

Equations (11), (12), (14) and (16) give

$$\sigma_{v,xy}=\left(\frac{3\Gamma\phi}{8r_0}\right)\sin 2\theta\,\frac{40(K+1)(1-K)}{3\chi_0(19K+16)(2K+3)}\left(\lambda_b^{\,2}-\lambda_b^{\,5}\right). \quad (17)$$

Equation (17) describes the time evolution of $\sigma_{v,xy}$ through the time evolution of λ_b, which can be calculated by Eq. (15).

Equation (17) predicts that $\sigma_{v,xy}$ is positive for mixtures with $K < 1$. This prediction is explained by the local flow during the retraction. Figure 2 illustrates the projection of the spheroidal droplets at t_1 (solid line) and at t_2 (dotted line) on the xy plane ($t_s < t_1 < t_2$). The open arrows and the arrows filled with oblique lines indicate the flow of the matrix in the vicinity of the interface, and the flow inside the droplet, respectively. Because of the retraction during $t_1 \rightarrow t_2$, compression in the X direction and elongation in the Y direction occur in the droplet. On the other hand, the matrix in the vicinity of the interface experiences elongation in the X direction at the tops of the major axis and compression in the Y direction at the tops of the minor axes owing to the constraint of the matrix fluid around. The local flows in the matrix and in the droplet should be canceled out in each direction since they totally vanish under the large step strains without average (macroscopic) flow. As a result, the summation of the stresses due to the Newtonian flow of both fluids can be elongation in the X direction and compression in the Y direction for mixtures with $K < 1$, since η_m is larger than η_d. This means $\sigma_{v,xy} > 0$, and this expectation agrees with the prediction by Eq. (17).

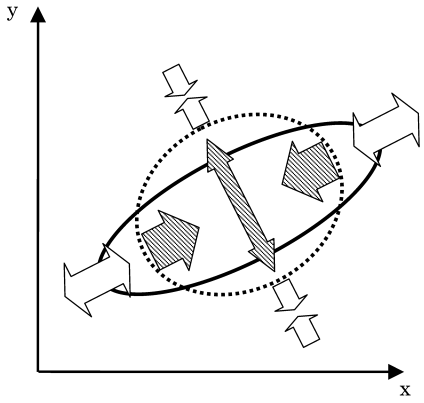

Fig. 2. Projection of a spheroidal droplet at t_1 (solid line) and t_2 (dotted line) on the xy plane during retraction ($t_s < t_1 < t_2$), showing compression and elongation of the droplet (arrows filled with oblique lines) and the matrix in the vicinity of the interface (open arrows).

2.3 Effects of Droplet Size Distribution

In our previous study,[10] droplet size distribution was incorporated into the expression for $\sigma_{L,xy}$. Here, we derive expressions for $\sigma_{v,xy}$ and $\sigma_{L,xy}$ at the last stage of the stress relaxation for blends with droplet size distribution. For the i-th droplet with radius r_i and volume fraction ϕ_i in a blend, the stress $(\sigma_{\xi,xy})_i$ can be written as

$$\left(\sigma_{\xi,xy}\right)_i = \left(\frac{3\Gamma\phi_i}{8r_i}\right)\sin 2\theta\; F_\xi\left[\lambda_b\left[\frac{t-t_s(r_i)}{\tau_D(r_i)}\right]\right], \quad (18)$$

where $\xi = v$ for the interface velocity term and $\xi = L$ for the Laplace pressure term. F_v and F_L are respectively determined by Eqs. (17) and (5), where λ_b is a function of $(t-t_s(r_i))/\tau_D(r_i)$ given by Eq. (15). The reduced time $t_s(r_i)/\tau_D(r_i)$ can be written as $t_s(r_i)/\tau_D(r_i) = t_s/\tau_D$, where t_s/τ_D is a function of γ and independent of r_i.[11] The r_i-independence of t_s/τ_D means that both t_s and τ_D are proportional to the droplet size. Provided that the interactions between the droplets are negligible, $\sigma_{\xi,xy}$ is given by the summation of Eq. (18) for all the droplets in the blend as follows:

$$\sigma_{\xi,xy} = \sum_{i=1}^{N}\left(\frac{3\Gamma\phi_i}{8r_i}\right)\sin 2\theta\; F_\xi\left[\lambda_b\left[\frac{t-t_s(r_i)}{\tau_D(r_i)}\right]\right], \quad (19)$$

where N denotes the total number of the droplets in the blend. Then, the reduced stress $(8r_V/3\Gamma\phi\sin 2\theta)\sigma_{\xi,xy}$ can be written as a function of reduced time $(t-t_s(r_V))/\tau_D(r_V)$

$$\left(8r_V/3\Gamma\phi\sin 2\theta\right)\sigma_{\xi,xy} = \sum_{i=1}^{N}\frac{r_V}{r_i}\frac{\phi_i}{\phi}F_\xi\left[\lambda_b\left[g\left(\frac{t-t_s(r_V)}{\tau_D(r_V)},\frac{r_V}{r_i},\gamma\right)\right]\right], \quad (20)$$

where r_V is the volume average radius defined by

$$r_V = \sum_{i=1}^{N} r_i^{\,4} \Big/ \sum_{i=1}^{N} r_i^{\,3}, \quad (21)$$

and the function g is given by

$$g\left(\frac{t-t_s(r_V)}{\tau_D(r_V)},\frac{r_V}{r_i},\gamma\right) = \left(\frac{r_V}{r_i}\right)\frac{t-t_s(r_V)}{\tau_D(r_V)} + \left(\frac{r_V}{r_i}-1\right)\frac{t_s}{\tau_D}, \quad (22)$$

where the relationship $t_s(r_i)/\tau_D(r_i) = t_s(r_V)/\tau_D(r_V) = t_s/\tau_D$ is used. Equation (22) shows that g is less than $(t - t_s(r_V))/\tau_D(r_V)$ for the droplets with $r_i > r_V$, and such droplets delay the stress relaxation. Moreover, Eq. (22) indicates that this delay is more significant at larger γ since t_s/τ_D increases with increasing γ.[11] As a result, non-linear behavior of the reduced stress can be predicted by Eq. (20) for the blends with droplet size distribution, in which the summation of F_ξ is made after the vertical shifts given by $(r_V/r_i)/(\phi_i/\phi)$ and the time shifts given by g are necessary.

3. COMPARISON WITH EXPERIMENTAL DATA

Figure 3 shows plots of the droplet Hencky strain $\ln(a/r_0)$ $(= \ln\lambda_a)$ versus $(t - t_s)/\tau_D$. Symbols show experimental results of the shape recovery in the last stage for the PIB droplets with different radii in a PDMS matrix ($K = 0.067$) at various step shear strains.[19,20] The solid line represents the calculated result by Eq. (15) with $\chi_0 = 0.110$.[11] The calculated result agrees well with the experimental data. From Eq. (13a), the slope of this line gives Λ_{XX}, and thus L_{XX} from Eq. (14). We can see from the slope of the solid line in Fig. 3 that $|\Lambda_{XX}|$ and $|L_{XX}|$ decrease with increasing $(t - t_s)/\tau_D$ and become zero at $(t - t_s)/\tau_D \to \infty$. This means that L_{YY} $(= -L_{XX}/2 > 0)$ and $\sigma_{v,xy}$ decrease with increasing $(t - t_s)/\tau_D$ and vanish at $(t - t_s)/\tau_D \to \infty$.

Figure 4 shows comparison between stress predictions and experimental data. The ordinate and the abscissa indicate the reduced stress $(8r_V/3\Gamma\phi\sin 2\theta)\sigma_{xy}$ and the reduced time $(t - t_s)/\tau_D$, respectively. Symbols denote the experimental data of the reduced stress relaxation curves under various large step shear strains for PIB/PDMS = 20/80 (wt/wt) blend[9] with $K = 0.081$ (with slightly different viscosities of components from those of the isolated droplet system). The solid and the broken lines indicate the reduced stress relaxation curves of $\sigma_{v,xy} + \sigma_{L,xy}$ and $\sigma_{L,xy}$ calculated by Eqs. (5), (15) and (17) with $r_0 = r_V$. To clarify the contribution of $\sigma_{v,xy}$, the time evolution of the ratio $\sigma_{v,xy}/(\sigma_{v,xy} + \sigma_{L,xy})$ is also shown by the dotted line. In the experimental results, θ is given by Eq. (6), τ_D is obtained from Eq. (12) substituting $r_0 = r_V$, and t_s/τ_D is determined by the relationship $t_s/\tau_D = 0.637\gamma^{1.82}$ based on the experimental data of the retraction.[11]

The reduced $\sigma_{L,xy}$ and the reduced $\sigma_{v,xy} + \sigma_{L,xy}$ decrease with increasing $(t - t_s)/\tau_D$. The total stress $\sigma_{v,xy} + \sigma_{L,xy}$ is larger than $\sigma_{L,xy}$ as a result of positive $\sigma_{v,xy}$. The ratio $\sigma_{v,xy}/(\sigma_{v,xy} + \sigma_{L,xy})$ increases with increasing $(t - t_s)/\tau_D$ and seems to be constant in the limits of $(t - t_s)/\tau_D \to 0$ and $(t - t_s)/\tau_D \to \infty$. An anonymous reviewer kindly pointed out that these limiting behaviors can be understood as follows. Expanding Eqs. (5) and (17) in powers of droplet strain ε, the reduced stress $\sigma_{L,xy}/(3\Gamma\phi\sin 2\theta/(8r_0))$ and $\lambda_b^2 - \lambda_b^5$ are respectively obtained as $\sigma_{L,xy}/(3\Gamma\phi\sin 2\theta/(8r_0)) = (16/5)\varepsilon$ and $\lambda_b^2 - \lambda_b^5 = (3/2)\varepsilon$ as far as terms of the first order, where $\lambda_a = 1 + \varepsilon$. This means that $\sigma_{v,xy}$ and $\sigma_{L,xy}$ are proportional to ε at $\varepsilon \to 0$. Therefore, $\sigma_{v,xy}/(\sigma_{v,xy} + \sigma_{L,xy})$ is independent of time and is given by a function of K at the end of the last stage. For $K = 0.081$, $\sigma_{v,xy}/(\sigma_{v,xy} + \sigma_{L,xy}) = 0.50$ is evaluated using the above relations. This agrees with $\sigma_{v,xy}/(\sigma_{v,xy} + \sigma_{L,xy})$ at $(t - t_s)/\tau_D = 10$ in Fig. 4. On the other hand, substituting $\lambda_a = \lambda_a(t_s) = 1.49$ into Eq. (5) and $\lambda_b = \{\lambda_a(t_s)\}^{-1/2} = 0.819$ into

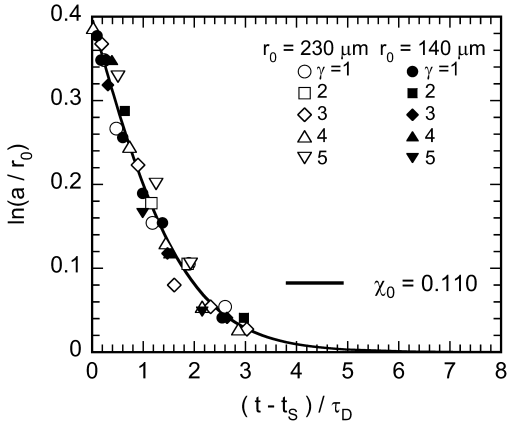

Fig. 3. Plots of the droplet Hencky strain $\ln(a/r_0)$ versus $(t - t_s)/\tau_D$. Symbols show experimental results for isolated PIB droplets with different radii in a PDMS matrix at various step shear strains γ. The solid line represents the calculated result of Eq. 15 with the constant $\chi_0 = 0.110$.

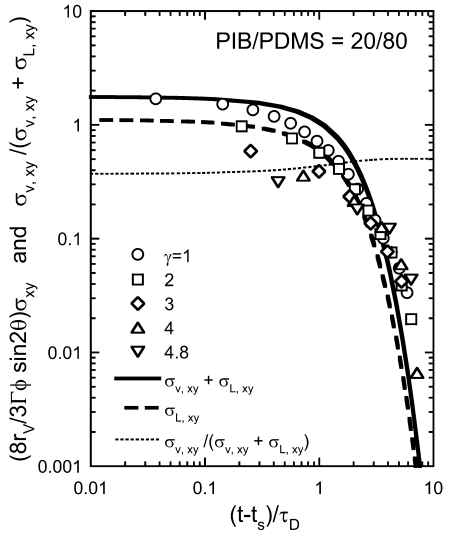

Fig. 4. Plots of reduced stress $(8r_V/3\Gamma\phi\sin 2\theta)\sigma_{xy}$ versus reduced time $(t - t_s(r_V))/\tau_D(r_V)$, and the ratio $\sigma_{v,xy}/(\sigma_{v,xy} + \sigma_{L,xy})$ versus $(t - t_s(r_V))/\tau_D(r_V)$. Lines show predicted contributions and symbols show the experimental results for the PIB/PDMS blend.

Eq. (17) yields $\sigma_{v,xy}/(\sigma_{v,xy}+\sigma_{L,xy}) = 0.37$ for $K = 0.081$ at $(t-t_s)/\tau_D = 0$. These results clearly show that $\sigma_{v,xy}$ is not negligible compared with $\sigma_{L,xy}$.

The calculated curves for $\sigma_{v,xy}$ and $\sigma_{v,xy}+\sigma_{L,xy}$ agree fairly well with the experimental results for the PIB/PDMS = 20/80 blend. However, closer look at the experimental data reveals that both of the magnitude and the decay rate of the reduced stress decreases with increasing γ. This result is different from the prediction, in which the reduced stresses are independent of γ. In order to explain the strain dependence of the reduced stress, other factors such as attractive interaction with adjacent droplets, droplet size distribution and uncertainty of t_s/τ_D in polydisperse system should be considered. The effects of these factors become weaker with decreasing γ. At $\gamma = 1$, $\sigma_{v,xy}+\sigma_{L,xy}$ is closer to the experimental data than $\sigma_{L,xy}$. It seems that $\sigma_{v,xy}$ as well as $\sigma_{L,xy}$ is essential to consider the stress due to the interface in blends.

Figure 5 shows the predicted curves of the reduced $\sigma_{v,xy}+\sigma_{L,xy}$ at various γ as functions of $(t-t_s(r_V))/\tau_D(r_V)$ calculated by Eq. (20) with Eqs. (5) and (17) assuming the model droplet size distribution in Table I. The polydispersity index r_V/r_n of the model distribution is $r_V/r_n = 1.20$, where r_n is the number average radius of droplets. This r_V/r_n value is chosen since the value is close to roughly estimated value of r_V/r_n for the PIB/PDMS blend.[10] We plot the calculated results only at $t \geq t_s(r_{max})$, where r_{max} denotes the radius for the largest droplet, since the largest droplet is not spheroidal shape at $t < t_s(r_{max})$, and thus the calculations at those times are out of the scope of the present paper.

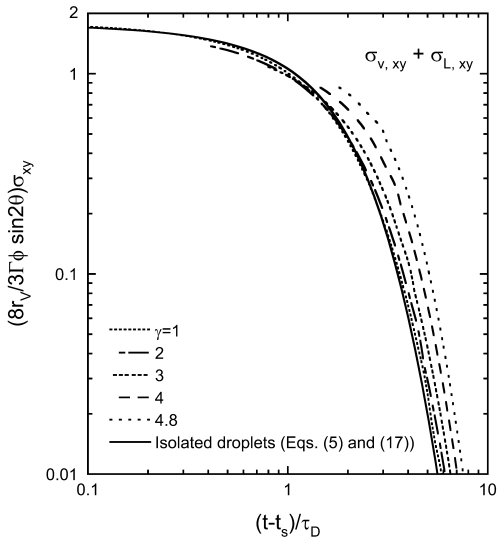

Fig. 5. Reduced stress $(8r_V/3\Gamma\phi\sin2\theta)\sigma_{xy}$ at various step shear strains γ calculated using the droplet size distribution in Table I as functions of reduced time $(t-t_s(r_V))/\tau_D(r_V)$.

In Fig. 5, the decay rate of the reduced stress decreases with increasing γ. As a result, the reduced stress increases with increasing γ at long times. The magnitude of the reduced stress at short times slightly decreases with increasing γ. These results qualitatively agree with the experimental results in Fig. 4 although the γ dependence are weaker than that of the experimental results for the PIB/PDMS blend. One reason of this quantitative disagreement may be the interactions between the dispersed droplets in the blend, which is neglected in Eq. (20). For the quantitative evaluation of the effect of the interactions, studies are necessary for blends with well-evaluated droplet size distributions.

4. CONCLUSIONS

Time evolution of total stress tensor for immiscible polymer blends is calculated in the last stage of the stress relaxation under large step shear strains as volume average of local stress tensor[1,2] using the time evolution of droplet shape, which is calculated by the theory for retraction of isolated droplets with spheroidal shape.[16] These theories are connected by the reduced velocity gradient of the droplet defined as the differentiation of the Hencky strain of the isolated droplets by the reduced time. In the last stage of the stress relaxation, the total stress tensor is given by the summation of the contributions from the motion of the interface (the interface velocity term) and the pressure difference beyond the interface (the Laplace pressure term). The calculated results are compared with the experimental data for a PIB/PDMS blend with the viscosity ratio $K = 0.081$.[9]

The interface velocity term for $K = 0.081$ is 37 % of the total stress at the beginning of the last stage and 50 % at the end. Therefore, this term is not negligible compared with the Laplace pressure term. The time evolution of the reduced stress calculated by the theories is independent of step shear strains γ, while the time evolution of the reduced stress

Table I. Model distribution of droplet size for the calculation shown in Fig. 5. f_i denotes the number fraction of i-th droplet.

i	f_i	r_i/r_n	r_i/r_V	ϕ_i/ϕ
1	0.25	0.600	0.498	0.0435
2	0.50	1.000	0.831	0.403
3	0.25	1.400	1.163	0.553

determined from the experimental data exhibits significant γ dependence. At $\gamma = 1$, in which effects inherent to polydisperse system (such as attractive interaction between adjacent droplets, droplet size distribution and uncertainty of the starting time of the last stage) is the smallest, the total stress (the summation of the interface velocity term and the Laplace pressure term) agrees well with the experimental data. This indicates that the interface velocity term is essential to predict the total stress tensor in immiscible polymer blends. The γ dependence of the reduced stress in the experimental data can be qualitatively explained by considering droplet size distribution in the theoretical calculation but there is still quantitative disagreement between the experimental data and the theoretical calculation. This disagreement may be caused by the interaction between adjacent droplets.

Acknowledgements

The valuable comments of the anonymous reviewer are gratefully acknowledged. This work was partially supported by a Grant-in-Aid for Scientific Research (B) No. 18350119 from the Japan Society for the Promotion of Science (JSPS).

REFERENCES

1) Batchelor GK, *J Fluid Mech* **41**, 545 (1970).
2) Mellema J, Willemse WM, *Physica*, **A122**, 286 (1983).
3) Onuki A, *Phys Rev A*, **35**, 5149 (1987).
4) Doi M, Ohta T, *J Chem Phys*, **95**, 1242 (1991).
5) Takahashi Y, Kurashima N, Noda I, Doi M, *J Rheol*, **38**, 699 (1994).
6) Takahashi Y, Kitade S, Kurashima N, Noda I, *Polym J (Tokyo)*, **26**, 1206 (1994).
7) Takahashi Y, Noda I, *"Flow-induced Structure in Polymers"*, Nakatani AI, Dadmun MD ed, (1995), American Chemical Society, Washington, DC, p 140.
8) Kitade S, Ichikawa A, Imura N, Takahashi Y, Noda I, *J Rheol*, **41**, 1039 (1997).
9) Okamoto K, Takahashi M, Watanabe H, Koyama K, Masuda T, *Proceeding of the International Conference on Advanced Polymer and Processing*, Yonezawa, 195 (2001).
10) Takahashi M, Macaubas PHP, Okamoto K, Jinnai H, Nishikawa Y, *Polymer*, **48**, 2371 (2007).
11) Takahashi M, Okamoto K, *Nihon Reoroji Gakkaishi (J Soc Rheol Jpn)*, **35**, 199 (2007).
12) Wetzel ED, Tucker III CL, *J Fluid Mech*, **426**, 199 (2001).
13) Yu W, Bousmina M, *J Rheol*, **47**, 1011 (2003).
14) Yu W, Bousmina M, Zhou C, Tucker III CL, *J Rheol*, **48**, 417 (2004).
15) Yu W, Zhou C, *J Rheol*, **51**, 179 (2007).
16) Okamoto K, Takahashi M, Yamane H, Watashiba H, Tsukahara Y, Masuda T, *Nihon Reoroji Gakkaishi (J Soc Rheol Jpn)*, **27**, 109 (1999).
17) Landau LD, Lifshitz EM, *"Fluid mechanics"*, 1st ed, (1959) Pergamon, Oxford, Chap 7.
18) Rosenkilde CE, *J Math Phys*, **8**, 84 (1967).
19) Yamane H, Takahashi M, Hayashi R, Okamoto K, Kashihara H, Masuda T, *J Rheol*, **42**, 567 (1998).
20) Hayashi R, Takahashi M, Yamane H, Jinnai H, Watanabe H, *Polymer*, **42**, 757 (2001).
21) Okamoto K, Takahashi M, Yamane H, Kashihara H, Watanabe H, Masuda T, *J Rheol*, **43**, 951 (1999).
22) Macaubas PHP, Kawamoto H, Takahashi M, Okamoto K, Takigawa T, *Rheol Acta*, **46**, 921 (2007).
23) Yu W, Bousmina M, Zhou C, *Rheol Acta*, **43**, 342 (2004).
24) Palierne JF, *Rheol Acta*, **29**, 204 (1990).
25) Graebling D, Muller R, Palierne JF, *Macromolecules*, **26**, 320 (1993).